Journal of Luminescence 215 (2019) 116613

Contents lists available at ScienceDirect

Journal of Luminescence

journal homepage: www.elsevier.com/locate/jlumin

Light yield of scintillating nanocrystals under X-ray and electron excitation

R.M. Turtos[a,*], S. Gundacker[a,c], S. Omelkov[b], E. Auffray[a], P. Lecoq[a]

[a] CERN, Geneva 23, CH, 1211, Switzerland
[b] Institute of Physics, University of Tartu, W. Ostwaldi Str.1, Tartu, 50411, Estonia
[c] Università Degli Studi di Milano Bicocca, Piazza Dell'Ateneo Nuovo 1, 20126, Milano, Italy

ARTICLE INFO

Keywords:
Fast timing
Scintillating nanocrystals
Light yield

ABSTRACT

In the field of fast timing research, direct-band-gap-engineered semiconductor nanostructures have shown high potential as a new source of prompt photon emission, different from Cherenkov and hot intraband luminescence. In these types of materials, quantum confinement of electron-hole pairs and coherent exciton states play a significant role in enhancing the dipole moment of the absorption and emission transitions. Thus they provide a sub-1 ns radiative decay component, critical to improve state-of-the-art time resolution of current bulk classical scintillators. However, the efficiency of this fast emission processes have not been determined so far in terms of number of photons emitted per energy deposited in the keV range. In this contribution, we propose several methods to determine the light yield of different nano-scintillating structures in order to understand their potential as radiation detectors for fast timing applications. These methods have been implemented using samples of a broad spectrum regarding synthesis, fabrication and preparation methods as well as registered scintillation efficiency, using both X-ray and electron excitation.

1. Introduction

In the search for a new generation of light-based radiation detectors, fast timing figures as one of the main drivers due to its outstanding impact in current particle detection techniques. State-of-the-art scintillators showing a coincidence time resolution (CTR) at the level of 50 ps [1] when detecting 511 keV gammas are able to convert energy from high energetic particles into optical photons at a maximum rate of at most of 1 photon per MeV per picosecond. The efficiency of this high-dynamical range wavelength shifting process reaches values of around 50% in the best cases. Therefore, for the next generation of materials with a photon emission rate suitable to improve the time resolution to the 10 ps level, a time contraction of the scintillating pulse constitutes a critical requirement. In terms of rise-, decay-times and light yield, one of the best and most used scintillators in time-of-flight positron emission tomography (TOF-PET) with one of the highest time photon density is $Lu_{(2-x)}Y_xSiO_5$ (LYSO:Ce). This material presents a rise time of about 50–70 ps, a decay time of 40 ns [2] and an intrinsic (absolute) light yield estimated to be 40′000 ph/MeV [3] measured with monochromatic electron excitation of 1 MeV. Electrons with this energy are minimum ionizing particles allowing a fair comparison between electron excitation yield and light yield under gamma excitation.

One of the first studies highlighting possible strategies to reach sub-100 ps values in time resolution with scintillating detectors [2] concluded that prompt photon emission added to the LYSO:Ce signal is a viable solution to decrease the overall timing jitter. Among them, Cherenkov and hot intraband luminescence are obvious candidates. However at present, both of them offer a low photon-emission yield of a few tens of ph/MeV, yet insufficient to impact the time resolution at the level of 10 ps [4].

The reasons described above lead us to investigate the timing performance of direct band gap engineered semiconductor nanocrystals [5]. In these types of materials, the quantum confinement of electron-hole pairs plays a significant role in enhancing the probability of radiative decay and it also allows for a excitonic and biexcitonic population stable at room temperature.

Previous results, obtained upon excitation of CdSe colloidal nanoplatelets (dimensions of 32 × 8x1.5 nm^3) [6] with X-rays up to 40 keV, found radioluminescent (RL) decay times at the level of 25 ps for around 25% of the photons. The second component of 300 ps was responsible for the rest 75% of the emission [5]. The overall RL spectra of CdSe nanoplatelets with 4–5 monolayers appears red-shifted when comparing to 370 nm laser excitation and centered at 530±10 nm, which was attributed to biexcitonic or multiexcitonic emission. These results have been confirmed by a cathodoluminescence (CL) study performed on the same type of nanoplatelets with different aspect ratios

* Corresponding author.
E-mail address: rosana.martinez.turtos@cern.ch (R.M. Turtos).

https://doi.org/10.1016/j.jlumin.2019.116613
Received 31 January 2019; Received in revised form 25 June 2019; Accepted 8 July 2019
Available online 13 July 2019

from 1:1 to 1:5 [7] using electrons of 120 keV. In this case, due to the higher signal-to-noise ratio of the CL setup, we were able to measure delayed excitonic emission with decay times longer than 300 ps, which accounts for 50% of the whole light output. The CL spectra also showed up red-shifted emission centered at 525±2 nm, independently of the aspect ratio of the nanoplatelets.

A logical step in the characterization of these new types of ultrafast nano-materials presenting very small Stokes shift would be the determination of the number of photons emitted per energy deposited, usually reported in ph/MeV. The light yield measurement would not only define the potential of these materials as ultrafast radiation detectors but also offer an extra parameter to understand the nature of the red-shifted RL and CL emission. However, the intrinsic geometrical features of nanocrystals or nanostructures impose several limitations on the amount of energy that can be deposited per single nanostructure and therefore lowers the number of photons to be measured. To mimic the scintillation process under the excitation conditions of 511 keV gamma rays as closely as possible, at least keV-range particles are required as irradiation source. Low energetic sources at the level of few keV stand a chance to be fully absorbed in nanostructured samples which are 100 nm thick, however light emission at such energies even for LYSO:Ce produces less than few hundreds photons and it is largely affected by non-proportionality. The low number of photoelectrons created at such low energies restricts the feasibility of measuring the light yield of nanostructures, except for those samples which are as efficient as LYSO:Ce in terms of photon emission. In view of this, a different way of determining the light yield must be applied.

In contrast to the conventional method, where a feature in the energy spectra, i.e. photopeak, Compton edge, etc. allows to correlate the number of photons produced per energy deposited, in this specific case we are forced to follow a different approach. For the case of X-ray excitation, the relation of number of photons emitted per energy deposited is obtained from two different measurements. The first aiming at measuring the light output of the nanostructures by comparing to the light output of known scintillating materials using a time-correlated single photon counting (TCSPC) method with a high detection efficiency. Then, a second measurement under the same excitation configuration but different readout determines the energy absorbed by the nanostructures through X-ray attenuation. For the case of electron excitation or cathodoluminescence, the light yield has been estimated by computing the ratio of the different emission bands (Ce centers and nanocrystals) obtained with a spectrograph calibrated for spectral sensitivity. The methodology followed and the results obtained are presented in the next sections.

2. Materials and methods

2.1. Built-up scintillating nano-layers

All the nanocrystals and nanostructures included in the study were chosen due to the presence of a sub-1ns decay component, which is critical for timing applications at the level of 10 ps [2].

Samples which are CdSe-based consist of 4 monolayers (ML) of CdSe in the form of nanoplatelets synthesized by wet chemical methods at the ILM[1] in Lyon, France following the protocol established in Ref. [8]. The main synthesis process is followed by a second step in order to provide the CdSe nanoplatelets with a CdS crown able to enhance their quantum yield and stability [9]. CdSe/CdS core crown nanoplatelets will be measured in the form of drop-casted films where each consecutive layer is deposited after solvent evaporation from the previous layer. To facilitate the formation of a dry drop-casted film, the final synthesis was followed by several steps where the ligand are washed and partially removed. This primitive deposition technique does not offer the best luminescence properties but it guarantees a built-up layer from which we can determine the light output lower limit. The films have been deposited on LYSO:Ce, glass or aluminium foil as the supportive substrate, which has been chosen in dependence of the type of measurement performed. The determination of the drop-casted film effective thickness is done assuming a homogeneous/bulk layer of CdSe taking into account the concentration of Cadmium atoms in solution and the volume deposited in a 3×3 mm^2 area [Private communication with B. Mahler from ILM, Lyon].

A second type of sample included in this study consists of ZnO:Ga dry nanopowders embedded in polystyrene by a hot-pressing method. In this case, the ZnO:Ga nanopowders were synthesized following several calcination processes in order to suppress defect band emission at the Czech Technical University in Prague, Czech Republic.[2] Meanwhile, the embedding procedure was carried out at the NUVIA company,[3] also based in Prague. This type of sample features a very interesting concept for the development of a new class of hybrid inorganic-organic scintillating material, where a polymer matrix is used to transfer non-radiative energy to the nano-emitters. ZnO:Ga has been added with a 10% weight in concentration and pressed down to form 1 mm thick sample as reported in Ref. [10]. A coincidence time resolution of 200 ps has been previously achieved and reported [11] when using 511 keV gamma excitation and single channel silicon photomultiplier (SiPM) readout. Despite the poor transparency of this sample and the modest values of time resolution achieved, we consider of most interest to understand the energy transfer mechanisms leading to photon emission in this type of system.

Another part of the current study will evaluate the photon-time density properties of a new type of material consisting of multiple InGaN/GaN quantum wells nanostructures grown by metalorganic vapour phase epitaxy (MOVPE) on a sapphire substrate. In this case, we will measure a sample consisting of 70 multiple quantum wells (MQW), equivalent to a 1.8 μm active region deposited on a 500 μm thick substrate [Private communication with A. Hospodková from FZU, Prague]. This type of nanostructures are fabricated at the Institute of Physics in Prague, Czech Republic.[4] Among all the samples, this one presents the best mechanical and optical properties due to the advanced method of fabrication. Further information about its fabrication process and luminescent properties can be found in Refs. [12–14].

2.2. Time-correlated single photon counting bench

The time-correlated single photon counting setup consists of a pulsed X-ray tube from Hamamatsu[5] and a hybrid PMT[6] connected through a constant fraction discriminator[7] to a fast TDC.[8] The fast TDC allows to record information from every single X-ray pulse and therefore, makes use of the high repetition rate provided by the laser.

The impulse response function (IRF) of the whole setup has been evaluated by convolving the characteristic time profile of every piece of the detector chain and was compared to the hot intraband luminescence (IBL) present in Li_2MoO_4. The IBL is a prompt emission (decay time <10 ps) [15], therefore the shape of obtained curve depends only on the instrumental response. The agreement between the IRF calculations and measurements is shown in Fig. 1. The calculated IRF and hot intraband luminescence time profile match almost exactly, except the pulse tail

[1] Institut Lumière Matière, Universitè Claude Bernard Lyon 1, http://ilm.univ-lyon1.fr.

[2] Faculty of Nuclear Sciences and Physical Engineering, https://www.cvut.cz.

[3] NUVIA, https://nuvia.cz.

[4] Institute of Physics of the Czech Academy of Science, https://www.fzu.cz.

[5] N5084 tungsten anode up to 40 kV with a time profile of 50ps FWHM.

[6] HPM-100-07 → https://www.becker-hickl.com/HPM-100.htm.

[7] ORTEC 9327 →https://www.ortec-online.com/products/electronics/amplifiers/9327.

[8] xTDC4-PCIe → http://www.cronologic.de/products/time-measurement/tdc/xtdc4/.

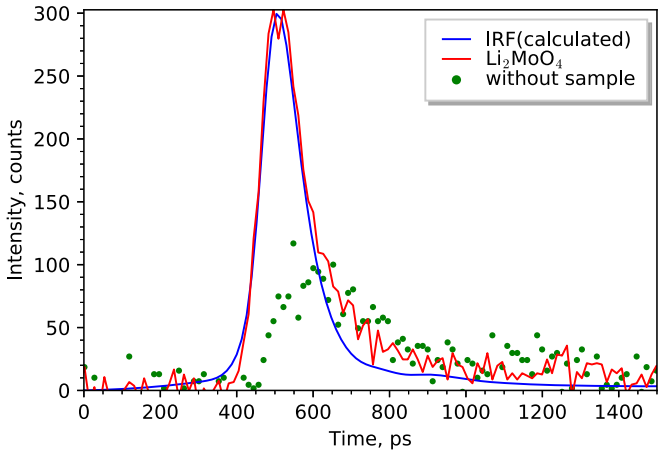

Fig. 1. Impulse response function of the TCSPC setup obtained by calculations and by recording the intraband luminescence of Li_2MoO_4 in the 220–850 nm spectral range.

where a ~0.5 ns component coming from the luminescence of air molecules [16] is visible. The latter is recorded separately by removing the sample.

The light output study is done by comparing the yield of nanostructures to the light collected from standard and well studied scintillating materials under the same excitation conditions. We use LYSO:Ce produced by Crystal Photonics, Inc. (CPI) and the plastic scintillator BC-422 from Saint-Gobain Ceramics & Plastics, Inc. (Saint Gobain) as reference samples. For the comparison between nanocrystal-based samples and standard scintillators, we take into account the reference's intrinsic light yield, i.e. 40′000 ph/MeV for LYSO:Ce [3] and we assume total energy deposition in the nanostructures. All samples are placed in the same position, excited with a X-ray beam collimated to 3 mm diameter (smaller than all samples) and readout in transmission mode using the same integration time window of 500 ns. A difficulty of this type of measurement is to ensure that the optical and geometrical characteristics are similar among the samples in comparison. In this regard, we assume that light travels through the nanocrystal-based samples in the same way than for the case of LYSO:Ce, a rather transparent material. Due to the small Stokes shift and higher self-absorption of direct band-gap semiconductors as CdSe or ZnO:Ga, this consideration most certainly underestimates the intrinsic light yield of nanocrystals. However, for the time being our aim is to asses the feasibility of the presented method and we will report light yield values based on this assumption as a lower bound.

2.3. X-ray attenuation

X-ray absorption by nanostructures is used to evaluate the energy deposited by X-rays in the samples under study. For this we use a LYSO:Ce $3 \times 3 \times 0.2\,mm^3$ thin plate readout by a Hamamatsu 3×3 mm^2 SiPM S13360 as detector, and we evaluate the difference of the X-ray tube energy spectra with and without nanocrystals in between X-rays and detector. The X-ray spectra extend up to 40 keV, with main lines centered at 8.4 keV and 9.7 keV together with a less intense line at 11.3 keV. As in the previous set of measurements, we perform all the data acquisition in single X-ray counting mode.

At first, we calibrate the detector by measuring the light yield of LYSO at the energy of the X-ray tube characteristic lines (around 9 keV). This allows to understand the possibility of measuring the light yield of nanocrystals directly by coupling them to the SiPM and looking at the shape of the energy spectra, i.e. X-rays lines.

The data taken with the LYSO + SiPM with and without nanocrystals is analyzed in order to report a value of mean energy deposited in the scintillating nanolayer, calculated as:

$$<E_{dep}^{NCs}> = <E_{dep}^{LYSO}> - <E_{dep}^{LYSO}>^{NCs} \quad (1)$$

Here $<E_{dep}^{LYSO}>$ refers to the mean energy deposited in the LYSO:Ce plate when the LYSO + SiPM detector is placed in front of the collimated X-ray beam. $<E_{dep}^{LYSO}>^{NCs}$ is the mean energy deposited when the nano-layers are placed between the X-ray tube and the LYSO + SiPM detector. For supplementary information on the determination of the mean energy deposited, please refer to Appendix A.

The fact that energy stopped by the built-up nano-layer does not precisely corresponds to energy deposited in the nanocrystals constitutes a technicality we are aware of. However, for now we have decided to consider them as the same, i.e. no energy escapes the nano-layer, since this approach offers a lower limit for the purpose of estimating light yield. Furthermore, the mean energy absorbed or "deposited" in the nano-layer has no relevance in terms of absolute values, because its determination depends on several parameters including energy resolution, noise level, trigger, etc. Therefore, we will use the mean energy deposited with and without nanocrystals to compute the ratio or efficiency of energy deposited in the nano-layer and we will use this parameter together with the light collected in the TCSPC measurement to give a final light yield estimation for the different nano-samples. The ratio of energy deposited is calculated according to the following relation:

$$\eta = \frac{<E_{dep}^{NCs}>}{<E_{dep}^{LYSO}>} = \frac{<E_{dep}^{LYSO}> - <E_{dep}^{LYSO}>^{NCs}}{<E_{dep}^{LYSO}>} \quad (2)$$

2.4. Cathodoluminescence setup

The CdSe-based samples were prepared by drop-casting the colloidal solution on top of a 3×3 mm^2 LYSO:Ce plate, 200 μm thick. The full absorption of the electron beam in the drop-casted nanoplatelets films is possible only at low-energies. The Monte-Carlo simulations (WinXray package [17]) indicated that 10 keV electron beam is fully absorbed in ~0.65 μm layer of bulk CdSe, while 5 keV beam penetrates only ~0.2 μm. The cathodoluminescence spectra and decay kinetics under continuous and pulsed low-energy excitation were obtained using a continuous monochromatic electron gun[9] with E_e^{max} = 10 keV. We used a somewhat defocused beam (>3×3 mm^2) to cover as much of the sample area as possible. Electron current was monitored by a ∅5 mm Faraday cup, and in the current experiment two values of current were used: 110 nA and 55 nA. An ARC Spectra Pro 2300i monochromator with a Hamamatsu H8259SEL photon counting head (dark count rate <3 cps) or an LN_2-cooled CCD camera were used as a registration system in the UV-visible range. To check for the full absorption conditions in the nanoplatelet layer, the emission decay kinetics was monitored to ensure no 40 ns component from the LYSO:Ce substrate is present. For that, we used the beam blanker which forms 10 ns wide square pulses with a repetition rate of 5 kHz. A Multiscaler card[10] was used for decay curve recording. It turned out that all the samples had uncoated parts near the edges of plates, however for samples >1 μm the impact of the substrate on the total yield of a sample was negligibly small. As a yield standard, an uncoated LYSO:Ce plate was used, which belongs to the same batch of plates used for the TCSPC and X-ray attenuation measurements. The continuous glow of the heated - Y_2O_3 cathode of the electron gun was not subtracted from the measured emission spectra, but below 600 nm it has negligible intensity [18]. All cathodoluminescence spectra were corrected for the spectral sensitivity of the respective detection systems. The correction method has been described in detail in Ref. [15].

For nanoparticles embedded in polystyrene a higher-energy electron beam with broad spectrum and E_e^{max} = 120 keV was used. In pure

[9] Kimball Physics EGG-3101.
[10] Becker&Hickl MSA-300.

Table 1
Comparative light output of different scintillating nanostructures measured in time correlated single photon counting mode over 500ns gate using a tungsten X-ray tube up to 40 keV, a standard LYSO:Ce crystal as main reference. Non-proportionality of LYSO:Ce at 10–40 keV energies is considered 55% [19].

Scint	*Light Output (%)*	η	$Yield^{*}_{1ns}$ (%)	$Yield^{*}_{10ns}$ (%)
LYSO:Ce (ref)	100	1	2.4	24
BC-422	33	1	53	98
PWO	0.6	1	30	90
Nanoscint	*Light Output (%)*	η_{sim}	$Yield_1$ (%)	$Yield^{*}_{10ns}$ (%)
InGaN/GaN 1.8 μm	2.3	0.036	30	70
CdSe/CdS NPLs 20 μm	0.5	0.4	60	75
ZnO:Ga@PS 1 mm	1.4	0.5	80	99

* The $Yield_{1ns}$ and $Yield_{10ns}$ represents the percentage of the emission integrated over 1 ns or 10 ns with respect to the total emission integrated over 500 ns.

polystyrene its penetration depth is less than 0.2 mm and samples are 1 mm thick. The spectra and decays were obtained at the pulsed cathodoluminescence setup described in Ref. [15]. The electron beam with 200 ps FWHM pulse and peak electron current of 0.7 or 10 A/cm^2 was used as source of excitation. The Andor iStar iCCD was used to obtain the gated spectra in different time windows. For decay curves, a Hamamatsu R3809U-50 MCP-PMT was used, with response of 250 ps FWHM. A total time window monitored after the excitation pulse was 50 μs. The instrumental response function (IRF) was determined by measuring the time profile of hot intraband luminescence (IBL) of PbF_2 single crystal.

3. Results

3.1. Comparative light output using TCSPC readout

A resume of the comparative light output measurements is presented in Table 1. In this case, the η_{sim} coefficient has been determined by Geant4 simulations in which we assume the nanostructures as an homogeneous layer of material with an effective thickness. In the case of InGaN/GaN, the calculations were done with 1.8 μm thick active layer followed by a sapphire substrate and for the CdSe/CdS drop-casted films we use the thickness equivalent to the amount of CdSe deposited in a 3 × 3 mm^2 area. That would be an equivalent to 20 μm homogeneous CdSe layer when depositing 100 μL from a solution with a Cadmium concentration of 4.4 g/L. For the case when the nanocrystals are embedded in polystyrene, a good compromise to understand the amount of energy deposited is to determine a mean density, calculated on the basis of the weight concentration of the nanocrystals in polystyrene. However this estimation does not allow to understand how much from the energy deposited in the host material is actually transferred to the nanocrystals. For the ZnO:Ga@PS sample we use a mean density of 1.5 g/cm^3 to calculate the η_{sim} value.

3.2. X-ray absorption by scintillating nanolayers

3.2.1. LYSO:Ce coupled to SiPM readout as X-ray detector

In order to understand the feasibility of using LYSO:Ce coupled to a SiPM to perform X-ray spectroscopy, we first evaluated the LYSO:Ce light output and looked at the number of photoelectrons detected per X-ray line. The X-ray tube energy spectra as measured with a LYSO:Ce 200 μm thick plate glued to a Hamamatsu SiPM (S13360-3050) and wrapped with one layer of Teflon is shown in Fig. 2. The experimental setup uses the laser clock to trigger the data acquisition. Charge is integrated within a 450 ns gate after each laser/X-ray pulse. The first peak centered at zero Vs, corresponds to either dark counts or X-ray pulses depositing no-energy in LYSO:Ce. The X-ray lines are resolved all together in one peak centered at around 20nV•s and due to the LYSO

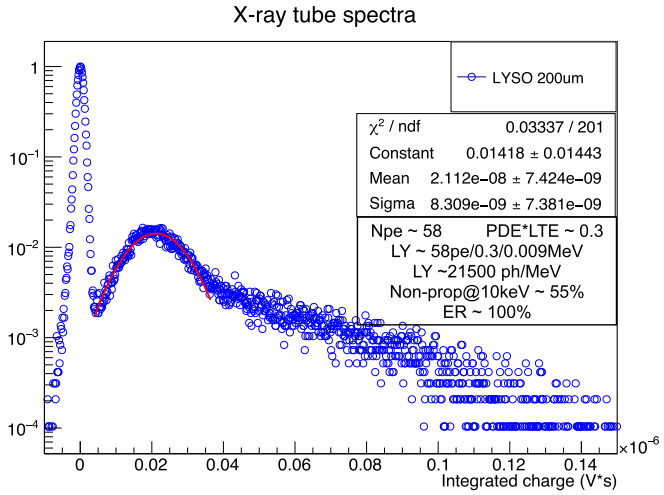

Fig. 2. 40 kV tungsten X-ray tube energy spectra as measured with a LYSO:Ce 3 × 3 × 0.2 mm^3 thin plate wrapped with one layer of Teflon and coupled to Hamamatsu 3 × 3 mm^3 SiPM. Single cell charge is 0.36 nV·s.

self-activation the spectra extends beyond 80 nV•s (equivalent to around 40 keV). The single cell charge is 0.36 nV•s, which results in around 58 photoelectrons at the X-ray lines. This level of signal sets severe limitations in determining lower values of light yield when measuring different materials, specially if they will be lower than LYSO:Ce by a factor 10 or 100 as suggested in Table 1.

From the light output values reported in Table 1, we can deduce that the only sample which could be used to measure directly the X-ray spectra is InGaN/GaN MQW. Fig. 3 (left) shows the comparative X-ray spectra as obtained with LYSO:Ce (green), InGaN/GaN MQW (red) and CdSe/CdS drop-casted film (blue) samples. Even though the energy resolution is extremely poor and the probability of X-rays interacting in a 1.8 μm thick InGaN/GaN active layer very low, there are few events yielding a light output as high as LYSO:Ce.

To cross check these results, we use an Fe^{55} electron source with energies up to 5 keV in order to confirm the light yield of InGaN/GaN multiple quantum wells nanostructures. Electrons up to 5 keV will be fully stopped in the InGaN/GaN active layer and light produced will be measured with the Hamamatsu SiPM. The energy spectra obtained after using a Fe^{55} source as excitation is shown to the right of Fig. 3. The peak of the LYSO:Ce spectra corresponding to 5 keV is centered at about 8 nV·s, i.e. 22 photoelectrons. This number is consistent with the 60 photoelectrons measured for the 8–9 keV X-ray lines when taking into account the energy difference and different wrapping configurations. In this case the LYSO:Ce plate is unwrapped to avoid the electrons stopping at the Teflon layer. InGaN/GaN light output is compared to LYSO:Ce (spectra in green) and BC-422 (spectra in blue), a plastic scintillator with a light output 3 times less than LYSO:Ce as confirmed by the electron energy spectra.

This test confirms that the InGaN/GaN sample has a light output as high as about 66% of that of LYSO:Ce and therefore carries a high potential for fast timing research. Converting to light yield values and assuming total energy deposition in the MeV range, InGaN/GaN has an estimated light yield of about 14′700 ph/MeV. This value considers LYSO:Ce with a light yield of about 22′000 ph/MeV when excited by electrons of 5 keV taking into account the non-proportionality factor at this energy [19].

For the other types of nanostructures based on CdSe/CdS and ZnO:Ga nanocrystals, we focus our effort in determining their energy absorption using the LYSO + SiPM readout as a X-ray detector. For this measurement, we use the X-ray absorption by different nano-scintillating samples to estimate the energy deposition ratio, factor η. The first step consists in the validation of the method by measuring X-ray absorption by aluminium thin foils (refer to Appendix A).

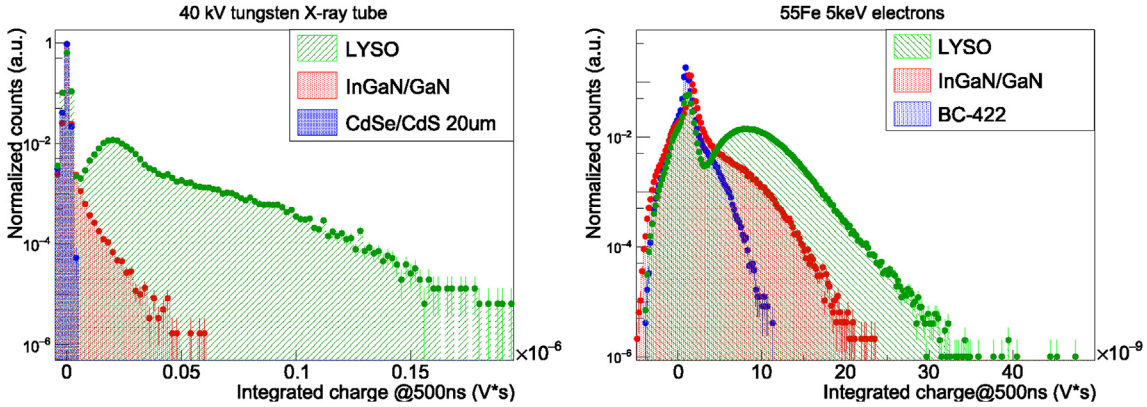

Fig. 3. Energy spectra as measured with a InGaN/GaN MQW deposited on sapphire substrate directly coupled to Hamamatsu 3 × 3 mm^2 SiPM in comparison to other standard and non-standard scintillators. Left: 40 kV tungsten X-ray tube used as excitation source. Right: Fe^{55} with 5 keV electrons used as excitation source. Single cell charge is 0.36 nV·s.

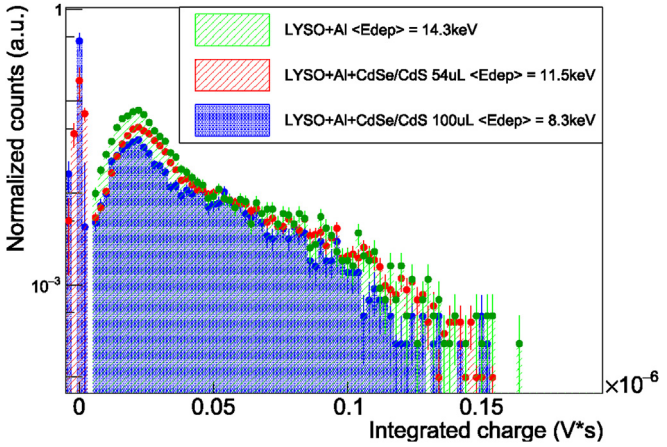

Fig. 4. X-ray attenuated by CdSe/CdS nanoplatelets drop-casted film with an equivalent thickness of 10 μm in comparison to 20 μm, readout by LYSO + SiPM.

The CdSe/CdS drop-casted films were deposited on an aluminium 3x3x0.016 μm^3 sheet, which covers the LYSO + SiPM detector and acts as the reflective layer all together. The measurements for the estimation of the energy deposited in the drop-casted nanocrystal layer are shown in Fig. 4. The 54 μL deposition should form a layer of around 10 μm and the second deposition would be 20 μm. The effective thickness is calculated by assuming an homogeneous deposition of nanocrystals taking into account the amount of CdSe used and dividing by the volume of the CdSe unit cell. As shown, the LYSO + SiPM readout seems to be sensitive enough to differentiate both nanocrystals layers yielding an η value of 0.4 for the 20 μm effective thick film.

3.2.2. Timepix chip readout as X-ray detector

The same calibration procedure using several layers of aluminium foil has been performed using a different detector, Timepix[11] chip from the Medipix collaboration at CERN [20]. In this detector, X-rays are directly converted to electrons in the 500 μm silicon substrate and the chip is designed to trigger in the signal itself at a level of 700pe, which cuts the X-ray spectra in the low energy part. In this case the difference in mean energy deposited between 0, 1 and 2 layers of aluminium roughly follows the simulated prediction yielding η values of 0.1 instead of 0.05. The results can be seen to the left hand side of Fig. 5. The mean energy deposited around 9 keV is lower than for the previous detector due to the silicon absorption coefficient which is smaller than for LYSO:Ce. Energy resolution for this detector is around 60% at the level of the X-ray lines, however as mentioned before this could be biased by the fact that we start measuring at around 2.5 keV.

The objective of this measurement is to validate the procedure followed with the LYSO + SiPM readout and cross-check results. To measure the same CdSe/CdS 100 μL drop-casted film readout with the LYSO + SiPM detector, we collimate the X-ray beam to a diameter of 3 mm because the Timepix chip is about 1.6 × 1.6 cm^2. The film is placed after the collimator, which ensures an homogeneous field exciting the nanocrystals. Results are shown at the right hand side of Fig. 5 where we compare the absorption of a nanocrystal layer deposited on an aluminium sheet to the absorption of only the aluminium foil.

The η value as obtained by this method is 0.36, which is in very good agreement with the 0.42 value obtained with the LYSO + SiPM readout and with the 0.5 value obtained by simulations. Due to the short acquisition time necessary to measure with the Timepix detector, we use it to determine the energy absorbed by the other sample.

A summary of the η factor obtained for the nano-scintillating samples is shown in Table 2, together with their final estimated values of light yield. We use the comparative light output results measured in the time correlated single photon counting setup and presented in Table 1 and divide them by the measured value of η to correct by the fact that all the energy is not dumped in the nano-layers. The light yield of LYSO:Ce used as reference is 22′000 ph/MeV, which takes into account a 55% non-proportionality at energies of 10 keV. For the case of electron excitation at 5 keV, we will assume the same level of non-proportionality.

As presented in Table 2, the estimated light yield values of materials like CdSe/CdS core crown nanoplatelets and ZnO:Ga@PS are indeed very modest, at the level of 275 ph/MeV and 500 ph/MeV respectively. Only the sample consisting of InGaN/GaN multiple quantum wells yields results comparable to LYSO:Ce of more than 10′000 ph/MeV. It's interesting to notice that the light yield LY_{sim} obtained when using the simulated η value from Table 1 is able to reproduce the measured values with good accuracy. The simulated η value has been obtained by treating the nanolayers as bulk material of an equivalent effective thickness, which seems to be accurate enough for the purpose of calculating the amount of energy deposited.

3.3. Low-energy cathodoluminescence yield of drop-casted CdSe/CdS films

Unfortunately, the CdSe/CdS drop-casted films have shown significant luminescence intensity degradation during continuous electron beam irradiation. At first, 10 keV, 110 nA beam was used to quickly record spectra of the samples introducing as small degradation as

[11] https://medipix.web.cern.ch/technology-chip/timepix-chip.

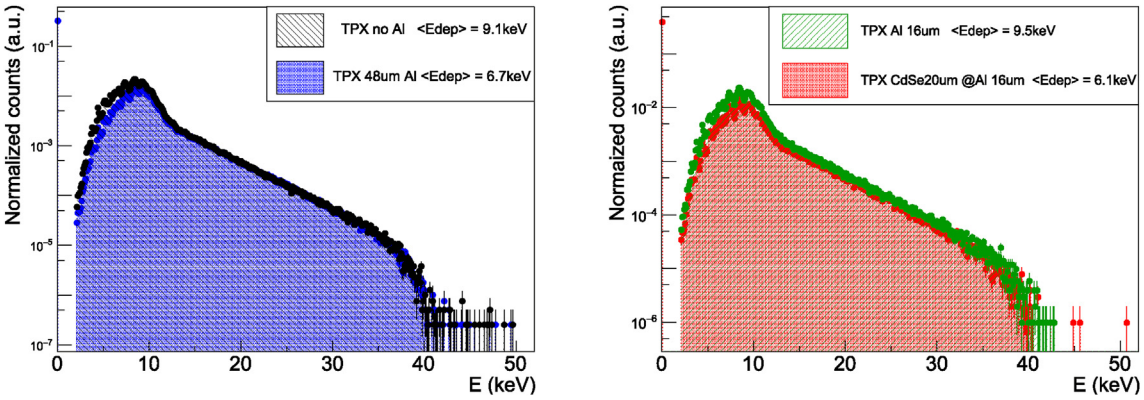

Fig. 5. X-ray tube energy spectra as measured with the Timepix chip. Left: X-ray absorption for several layers of aluminium. Right: X-ray spectra attenuated by CdSe/CdS 20 μm thick drop-casted film.

Table 2
Measured absorption coefficient η and estimated light yield (ph/MeV) for different nano-scintillating samples obtained by the indirect and direct method under X-ray and electron excitation.

Nano-scint	*X-ray attenuation*			*Geant4 sim.*	*CL*[a]
	$\eta_{LYSO+SiPM}$	η_{TPX}	LY_{meas} *(ph/MeV)*	LY_{sim}	LY_{meas}
CdSe/CdS 20 μm	0.42	0.36	275	256	200
ZnO:Ga@PS 1 mm	–	0.60	500	610	634
Direct e- excitation					
InGaN/GaN 1.8 μm	→		14′700	14′000	–

[a] The cathodoluminescence results are presented in the next sections but summarized here for the purpose of comparison.

possible (Fig. 6 left, curve 1). At second, the experiment was repeated multiple times with 5 keV, 110 nA beam, recording evolution of the spectra during degradation (curves 2a–2c). Finally, a temporal evolution of the luminescence signal was recorded with 5 keV, 55 nA beam (Fig. 6 right), which follows hyperbolic power-law after the first few tens of seconds. The signal degradation is not recovered by keeping samples in the darkness for several hours. The low-energy CL emission spectrum appears the most red-shifted when comparing to laser and X-ray excitation, peaking at 540±10 nm. The yield integral under curve 1 above 485 nm is 0.96% of total LYSO:Ce yield integral.

Due to the rapid degradation of the samples it is hard to assess the NPLs yield accurately, it is only possible to give a lower boundary. One has to be careful to take into account non-proportionality of LYSO:Ce, which is 55% at 10 keV X-ray relative to the yield at 662 keV [19]. The exact yield under 10 keV electron beam might be different, but we can take the same value of 55% for the estimation. If the LYSO:Ce yield at 662 keV is 40′000 ph/MeV [3], we obtain cathodoluminescence yield value of 200 ph/MeV for 6 μm-effective-thick deposited nanoplatelet films. Given the difficulties of this experiment, this result seems to be in a good agreement with 275 ph/MeV obtained for X-ray excitation (see Table 2).

3.4. High-energy pulsed cathodoluminescence of ZnO:Ga@PS 10%

The procedure of pulsed CL yield comparison of transparent samples (crystals or polystyrene slabs) was described in Ref. [4]. The samples of ZnO:Ga@PS and LYSO:Ce were installed on the sample holder, and covered by identical aluminum masks to expose the same sample surface area (about 4×8 mm^2) to the wide homogeneous electron beam. Either of the samples could be positioned in front of the beam by the means of the manipulator, which enables precise comparison of the sample light output in the same conditions. However the ZnO:Ga@PS sample was opaque, which implies different light conversion efficiency as compared to transparent LYSO:Ce reference sample and respective inaccuracy in the yield estimation of the former. Fig. 7 shows the spectra of ZnO:Ga@PS and LYSO:Ce, recorded in 0–200 µs time window in the same conditions. Such time window was selected to ensure that all the luminescence has completely decayed during acquisition, so that the total yield of different emissions can be compared. The spectrum consists of three separate emission bands: polystyrene host luminescence at 330 nm, ZnO:Ga excitonic band at 390 nm and weak broad defect emission at ~530 nm. The absence of the latter in the spectrum recorded in 0–32 ns time window indicates that it has the decay constant in microsecond range.

The approximate yield numbers can be derived from integrating the spectra from Fig. 7. The total light yield of 390 nm excitonic band in

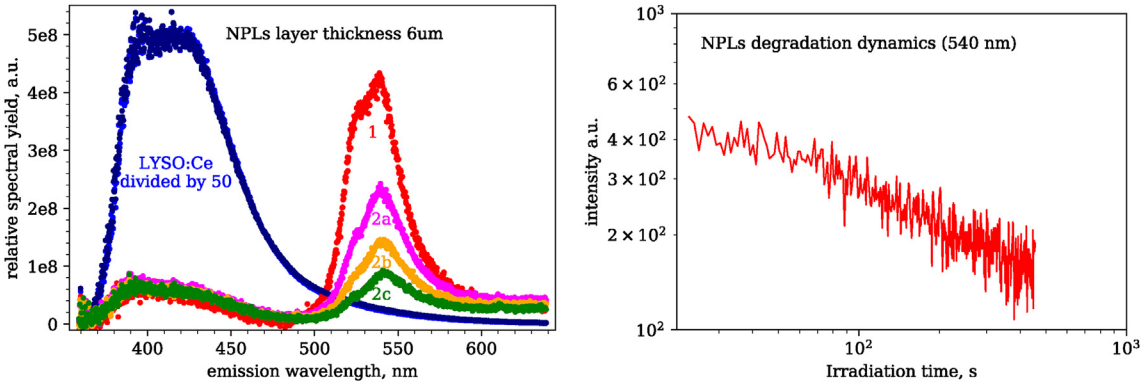

Fig. 6. The low-energy CL spectra of 6 μm-thick nanoplatelet layer recorded during the CL experiment (phase 1 and 2a-2c), in comparison to the uncoated LYSO:Ce plate, recorded in the same conditions (left). CL degradation curve of 2 μm-thick nanoplatelet layer, normalized arbitrarily (right).

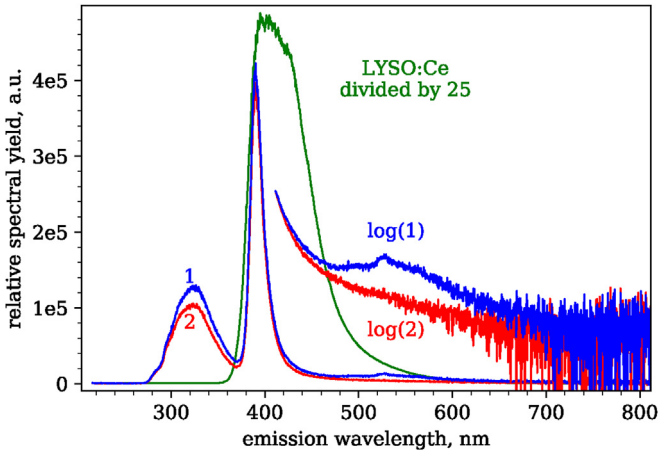

Fig. 7. The high-energy CL spectra of ZnO:Ga@PS 10% in the full (0–200 μs, curve 1) and fast (0–32 ns, curve 2) time windows, and their high-wavelength parts in logarithmic scale. The spectrum of LYSO:Ce, recorded in the same conditions in the 0–200 μs time window, is shown for comparison.

0–200 μs time window, integrated over 370–450 nm spectral region, is 0.92% of total LYSO:Ce cathodoluminescence yield. The non-proportionality of LYSO:Ce at 100–120 keV X-ray is 80–85% relative to the yield at 662 keV [19]. Assuming the same non-proportionality factor for the electron beam, the excitonic emission yield is 315 ph/MeV. For comparison, the yield of polystyrene and defect emission bands is 0.71% and 0.22% of LYSO:Ce, which comprise 38% and 12% of total light output of ZnO:Ga@PS. The total CL light output of ZnO:Ga@PS 10% is 634 ph/MeV. Contrary to electron beam, which penetrates a relatively thin layer of material (<0.2 mm for 120 keV), in the experiments with X-rays and gamma-excitation the bulk of nanocomposite is excited. Due to re-absorption by nanoparticles, the polystyrene intrinsic emission might not exit the sample altogether, which explains the lower total yield value of ZnO:Ga@PS obtained in the X-ray experiment (Table 2).

3.5. Discussion

From all the samples measured, CdSe-based colloidal nanocrystals in the shape of drop-casted dry films are the materials with the smallest light yield, similar to PWO of about 200 ph/MeV. However, their excellent timing performance with a sub-1ns decay time of around 300ps [5] (τ_{d1} = 20ps, 27%, τ_{d2} = 360ps, 41% and the rest 32% corresponds to a slower emission of > 4ns), its high biexciton binding energy together with a very low threshold for stimulated emission [6] place this type of nanocrystals in the list of materials for future applications. These results are encouraging since they assume that the light is not self-absorbed within the 20 μm effective thick layer. Therefore, they serve as starting point to improve the sample preparation and deposition method of CdSe-based nano-scintillating layers. A different way to create films allowing a better extraction of the light and guarantying the surface passivation of the nanoplatelets would highly improve the potential of these type of materials. An in-dept study of the dosimetric properties of CdSe-based nanoparticles can be found here [21–23].

One very interesting system from the energy transfer point of view are nanocrystals embedded in a host matrix, where the nanocrystals could be used to harvest the energy deposited in the matrix. We have studied polystyrene as a host material, even if, ideally, the density of this host matrix should be as high as possible to provide the necessary stopping power for energetic ionizing radiation. In this regard, the nanocrystals will act as the “fluors” or the activators added to plastic scintillators to boost the light yield by a factor 100. Ideally, the matrix would perform as the stopper and energy distributor and if the distances between the nanocrystals are smaller than the diffusion length of the excitons in the polymer, the emission centers could be efficiently excited. However, embedding colloidal nanoparticles into a polymer matrix requires a correct monodispersion and further functionalization of the ligands able to maintain the nanocrystals’ photoluminescence properties.

A different type of nanocrystals synthesized by UV irradiation instead of by wet chemistry is ZnO:Ga dry nanopowders. When they are embedded in polystyrene, the sample presents a light output of around 500 ph/MeV which explains the relatively modest time resolution measured previously and reported in Ref. [11]. This low light yield is signature of the high re-absorption and possibly low quantum yield of individual nanoparticles.

The best light yield result is obtained with the InGaN/GaN MQW sample (τ_{d1} = 800ps, 34%, τ_{d2} = 3.2ns, 43% and the rest 23% corresponds to a slow emission of several tenths of nanoseconds), which shows light output values at the level of LYSO:Ce. For this case, we are able to directly measure its light output by correlating the energy spectra of a 5 keV electron source to the number of photoelectrons detected. We can observe a discrepancy of around 5% between the value obtained by direct measurement with an electron source and the value estimated under X-rays excitation with the TCSPC setup. Due to the presence of the sapphire substrate this type of sample can not be used to determine the η value by measurements as done with CdSe-based and ZnO:Ga@PS samples. The future implementation of InGaN/GaN multiple quantum wells as radiation detectors will be further discussed in oncoming publications.

4. Conclusions

In this contribution, we have developed a new method to determine the light yield of different nano-scintillating structures in order to understand their potential as radiation detectors for fast timing applications. The method has been implemented using samples featuring a broad spectrum regarding fabrication and preparation methods as well as scintillation efficiency. Our approach uses two different readouts to measure separately light output and energy absorbed by the nanostructures. Light output is measured in time correlated single photon counting mode and energy absorption is determined with two different setups. The first one uses a thin plate of LYSO:Ce coupled to a Hamamatsu SiPM and the second employs the Timepix chip, which is able to directly convert X-rays to an electrical signal. Both readouts were proven to yield the same results and they were validated by using thin aluminium sheets as a reference material.

The new methodology following X-ray excitation has been cross checked using a completely different setup and type of excitation. Spectral and time resolved low-energy cathodoluminescence (E_{exc} = 10 keV) has been used to determine the yield of drop-casted CdSe/CdS core crown nanoplatelets films, while high-energy cathodoluminescence (E_{exc}^{max} = 120 keV) was used for polystyrene-based nanocomposites. The first results for CdSe-based films reveal the yields of around 200 ph/MeV, which compares to the 275 ph/MeV found under X-ray excitation. The causes for the degradation of the cathodoluminescence spectra after the first irradiation, is a topic that deserves a deep future investigation due to its possibly multi-parametric nature. However, the degradation effect has not been observed using X-ray or 511 keV gamma excitation and it is most probable highly correlated to the deposition technique of drop-casted films.

We have demonstrated the fact that we have a tool for light yield characterization of scintillating nano-structures and this sets an starting point for the future improvement of these type of nanocrystalline materials. On top, the cathodoluminescence setup also offers a powerful tool to look into the energy transfer mechanisms taking place when these nanocrystals are embedded in a matrix host able to redistribute the energy deposited.

From all the tested sampled only InGaN/GaN multiple quantum wells gives light yield results comparable to standard LYSO:Ce.

However the nanofabrication technique has limited built-up thickness and the total amount of energy that can be deposited is around 5–10 keV.

We consider this research as a significant step forward in the characterization of nano-scintillating materials for future time-of-flight applications.

Acknowledgments

The authors would like to strongly acknowledge the work of B. Mahler from the ILM in Lyon, for the synthesis of the CdSe/CdS core crown nanoplatelets in colloidal solution used in this study. As well as C. Dujardin for welcoming us at the Institute of Light and Matter, the group of V. Čuba at the Czech Technical University in Prague for the production of ZnO:Ga embedded in polystyrene and the group of A. Hospodková and Martin Nikl at the Institute of the Physics of the Czech Academy of Sciences for the fabrication of InGaN/GaN multiple quantum wells sample.

We are also most thankful for the collaboration maintained with the Medipix group at CERN, specially for the help of Lukas Tlustos and Jerome Alozy regarding technical support and the detector energy calibration.

This work was supported by ERC Advanced Grant no. 338953 (TICAL) and Estonian Research Council (projects PUT1081, IUT2-26). A partial financial support from the Estonian Centre of Excellence TK141 by the EU through the European Regional Development Fund (TK141, project No. 2014-2020.4.01.15-0011) is gratefully acknowledged. The research have been developed in the frame of the Crystal Clear Collaboration, the FAST Cost Action TD1401 and ASCIMAT project grant agreement no. 690599.

Appendix A. Validation of the X-ray absorption measurements using Aluminium thin foils

Fig. A.8 shows the difference in the mean energy deposited when having one layer of aluminium foil in between the X-rays and the LYSO + SiPM detector. Simulations are performed with the same geometric features than in the experiment using a X-ray spectra also obtained by simulations. The X-rays characteristic lines at 8.4 keV, 9.7–9.96 keV and 11.3 keV are well known, however the low energy part of the spectra which is determined by the Beryllium window and other filters could be different to the X-ray tube in use. In this case, both simulations and measurements are in well agreement showing a η value of around 0.06 and 0.07, respectively.

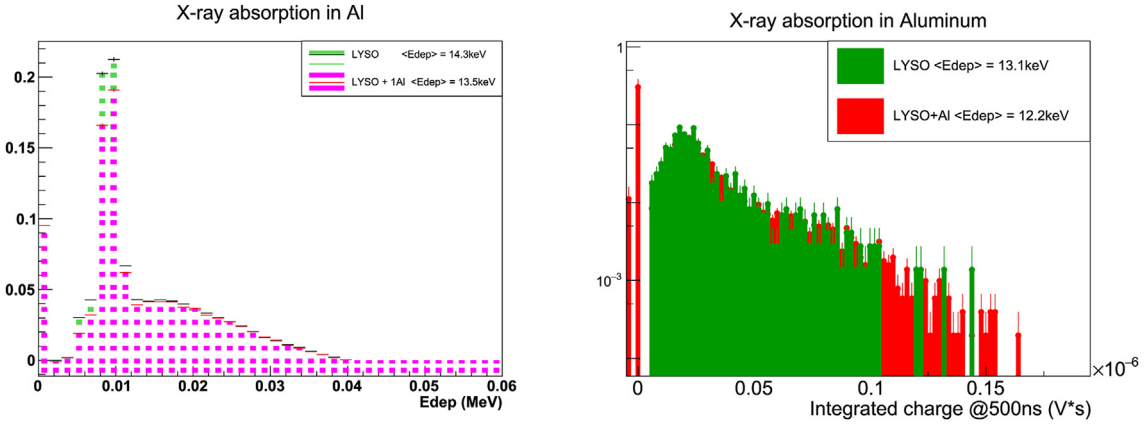

Fig. A.8. X-ray attenuation by an aluminium sheet 16 μm thick in comparison to one layer of teflon as obtained by Geant4 simulations (left) and measurements (right).

Mean energies are calculated following the equation $\langle x \rangle = \frac{\int x * f(x) dx}{\int f(x) dx}$. The bin of zero energy or zero counts is of most importance and in this case since we trigger on the laser clock, it is filled out with the difference in numbers of counts for each spectra under comparison.

Another test for validation aims to repeat the measurement but this time comparing 1 to 2 layers of aluminium. In this case, simulations predict a difference in mean energy deposited which corresponds to an η value equal to 0.05 as shown in Fig. A.9. The measurements for one or two foil of aluminium are shown to the right of Fig. A.9. The η value obtained by measurement is 0.06 so this allow us to move forward and estimate the energy absorbed in nanocrystals. The drop-casted films are deposited on an aluminium sheet which covers the SiPM and acts as reflective layer all together.

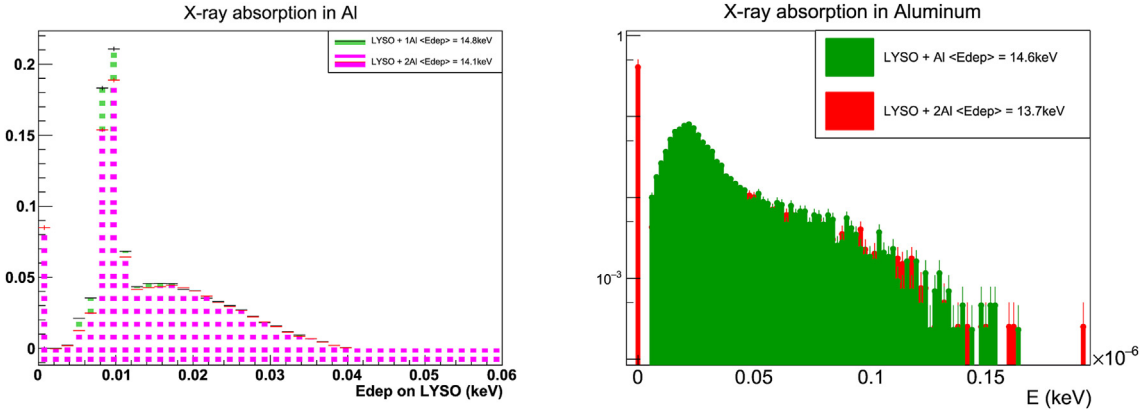

Fig. A.9. X-ray attenuation by an aluminium sheet 16 μm thick in comparison to 32 μm, i.e. 1 or 2 layers as obtained by Geant4 simulations (left) and measurements (right).2

Appendix B. Supplementary data

Supplementary data to this article can be found online at https://doi.org/10.1016/j.jlumin.2019.116613.

References

[1] S. Gundacker, R.M. Turtos, E. Auffray, M. Paganoni, P. Lecoq, High-frequency SiPM readout advances measured coincidence time resolution limits in TOF-PET, Phys. Med. Biol. 64 (5) (2019) 055012, https://doi.org/10.1088/1361-6560/aafd52 URL http://doi.org/10.1088/1361-6560/aafd52.

[2] S. Gundacker, E. Auffray, K. Pauwels, P. Lecoq, Measurement of intrinsic rise times for various L(Y)SO and LuAG scintillators with a general study of prompt photons to achieve 10 ps in TOF-PET, Phys. Med. Biol. 61 (7) (2016) 2802 URL http://stacks.iop.org/0031-9155/61/i=7/a=2802.

[3] R.M. Turtos, S. Gundacker, M. Pizzichemi, A. Ghezzi, K. Pauwels, E. Auffray, P. Lecoq, M. Paganoni, Measurement of LYSO intrinsic light yield using electron excitation, IEEE Trans. Nucl. Sci. 63 (2) (2016) 475–479 https://doi.org/10.1109/TNS.2016.2527738.

[4] S.I. Omelkov, V. Nagirnyi, S. Gundacker, D.A. Spassky, E. Auffray, P. Lecoq, M. Kirm, Scintillation yield of hot intraband luminescence, J. Lumin. 198 (2018) 260–271 https://doi.org/10.1016/j.jlumin.2018.02.027.

[5] R.M. Turtos, S. Gundacker, A. Polovitsyn, S. Christodoulou, M. Salomoni, E. Auffray, I. Moreels, P. Lecoq, J. Grim, Ultrafast emission from colloidal nanocrystals under pulsed x-ray excitation, J. Instrum. 11 (10) (2016) P10015 URL http://stacks.iop.org/1748-0221/11/i=10/a=P10015.

[6] J.Q. Grim, S. Christodoulou, F.D. Stasio, R. Krahne, R. Cingolani, L. Manna, I. Moreels, Continuous-wave biexciton lasing at room temperature using solution-processed quantum wells, Nat. Nanotechnol. 9 (2014) 891–895 https://doi.org/10.1038/NNANO.2014.213.

[7] R.M. Turtos, Electron Excited Emission of CdSe Nanoplatelets with Different Aspect Ratios, Short Scientific Term Report in the Frame of FAST Cost Action TD1401 at the Institute of Physics, Tartu University, September 2017.

[8] S. Ithurria, M.D. Tessier, B. Mahler, R.P.S.M. Lobo, B. Dubertret and A.L. Efros, Colloidal nanoplatelets with two-dimensional electronic structure, 10.1038/nmat3145. Nat. Mater. 10 (12) (2011) 936 URL https://doi.org/10.1038/nmat3145.

[9] M.D. Tessier, P. Spinicelli, D. Dupont, G. Patriarche, S. Ithurria, B. Dubertret, Efficient exciton concentrators built from colloidal core/crown cdse/cds semiconductor nanoplatelets, Nano Lett. 14 (1) (2014) 207–213 URL http://doi.org/10.1021/nl403746p.

[10] H. Burešová, L. Procházková, R.M. Turtos, V. Jarý, E. Mihóková, A. Beitlerová, R. Pjatkan, S. Gundacker, E. Auffray, P. Lecoq, M. Nikl, V. Čuba, Preparation and luminescence properties of ZnO-Ga- polystyrene composite scintillator, Opt. Express 24 (14) (2016) 15289–15298, https://doi.org/10.1364/OE.24.015289 URL http://www.opticsexpress.org/abstract.cfm?URI=oe-24-14-15289.

[11] R.M. Turtos, S. Gundacker, M.T. Lucchini, L. Procházková, V. Čubaba, H. Burešová, J. Mrázek, M. Nikl, P. Lecoq, E. Auffray, Timing performance of ZnO-Ga nanopowder composite scintillators, Phys. Status Solidi Rapid Res. Lett. 10 (11) (2016) 843–847, https://doi.org/10.1002/pssr.201600288 URL https://onlinelibrary.wiley.com/doi/pdf/10.1002/pssr.201600288.

[12] A. Hospodková, M. Nikl, O. Pacherová, J. Oswald, P. Brůža, D. Pànek, B. Foltynski, E. Hulicius, A. Beitlerová, M. Heuken, InGaN/GaN multiple quantum well for fast scintillation application: radioluminescence and photoluminescence study, Nanotechnology 25 (45) (2014) 455501 URL http://stacks.iop.org/0957-4484/25/i=45/a=455501.

[13] A. Hospodková, T. Hubáček, J. Oswald, J. Pangrác, K. Kuldová, M. Hývl, F. Dominec, G. Ledoux, C. Dujardin, InGaN/GaN structures: effect of the quantum well number on the cathodoluminescent properties, Phys. Status Solidi 255 (5) (2017) 1700464, https://doi.org/10.1002/pssb.201700464 arXiv https://onlinelibrary.wiley.com/doi/pdf/10.1002/pssb.201700464.

[14] T. Hubáček, A. Hospodková, K. Kuldová, J. Oswald, J. Pangrác, V. Jarý, F. Dominec, M. Slavická Zíková, F. Hájek, E. Hulicius, A. Vetushka, G. Ledoux, C. Dujardin, M. Nikl, Advancement toward ultra-thick and bright InGaN/GaN structures with a high number of QWs, CrystEngComm 21 (2019) 356–362 https://doi.org/10.1039/C8CE01830H.

[15] S. Omelkov, V. Nagirnyi, A. Vasil'ev, M. Kirm, New features of hot intraband luminescence for fast timing, J. Lumin. 176 (2016) 309–317 URL https://doi.org/10.1016/j.jlumin.2016.03.039.

[16] F. de Chaffaut, The luminescence decay time of air and nitrogen-oxygen mixtures excited by alpha particles, IEEE Trans. Nucl. Sci. 19 (3) (1972) 112–118, https://doi.org/10.1109/TNS.1972.4326710.

[17] R. Gauvin, E. Lifshin, H. Demers, P. Horny, H. Campbell, WinXray: a new Monte Carlo program that computes x-ray spectra obtained with a scanning electron microscope, Microsc. Microanal. 12 (2006) 49–64, https://doi.org/10.1017/S1431927606060089.

[18] S.I. Omelkov, V. Nagirnyi, E. Feldbach, R.M. Turtos, E. Auffray, M. Kirm, P. Lecoq, Intraband luminescence excited in new ways: low-power x-ray and electron beams, J. Lumin. 191 (2017) 61–67 URL https://doi.org/10.1016/j.jlumin.2017.02.001.

[19] C. Wanarak, W. Chewpraditkul, A. Phunpueok, Light yield non-proportionality and energy resolution of lu1.95y0.05sio5:ce and lu2sio5:ce scintillation crystals, Procedia Eng. 32 (2012) 765–771 iSEEC. doi https://doi.org/10.1016/j.proeng.2012.02.010.

[20] T. Poikela, J. Plosila, T. Westerlund, M. Campbell, M.D. Gaspari, X. Llopart, V. Gromov, R. Kluit, M. van Beuzekom, F. Zappon, V. Zivkovic, C. Brezina, K. Desch, Y. Fu, A. Kruth, Timepix3: a 65k channel hybrid pixel readout chip with simultaneous ToA/ToT and sparse readout, J. Instrum. 9 (05) (2014), https://doi.org/10.1088/1748-0221/9/05/c05013 C05013–C05013.

[21] M. Delage, M. Lecavalier, E. Cloutier, D. Larivière, C.N. Allen, L. Beaulieu, Robust shell passivation of CdSe colloidal quantum dots to stabilize radioluminescence emission, AIP Adv. 6 (10) (2016) 105011, https://doi.org/10.1063/1.4966144.

[22] M. Delage, M. Lecavalier, D. Larivière, C.N. Allen, L. Beaulieu, Characterization of a binary system composed of luminescent quantum dots for liquid scintillation, Phys. Med. Biol. 63 (17) (2018) 175012 https://doi.org/10.1088/1361-6560/aad9c3.

[23] M. Delage, M. Lecavalier, D. Larivière, C.N. Allen, L. Beaulieu, Dosimetric properties of colloidal quantum dot-based systems for scintillation dosimetry, Phys. Med. Biol. 64 (9) (2019) 095027, https://doi.org/10.1088/1361-6560/ab109b https://doi.org/10.1088/1361-6560/ab109b.